SCIENTIFIC JOURNAL
EARTH'S CRYOSPHERE

Earth's Cryosphere, 2015, vol. XIX, No. 4, pp. 36–47 **http://earthcryosphere.ru/**

PERIGLACIAL PROCESSES AND LANDFORMS

MULTISTAGE HOLOCENE MASSIVE ICE NEAR THE SABETTAYAKHA RIVER MOUTH, YAMAL PENINSULA

Yu.K. Vasil'chuk, N.A. Budantseva, A.C. Vasil'chuk, Ye.Ye. Podborny*, A.N. Sullina*, Ju.N. Chizhova

Lomonosov Moscow State University, Geography and Geology Departments, 1 Leninskie Gory, Moscow, 119991, Russia; vasilch_geo@mail.ru
**Hydroecological Research Center, 16A Nalichnaya str., St. Petersburg, 199406, Russia; epodbornyy@yandex.ru*

A unique case of Holocene massive ground ice on the Ob Gulf coast has been studied in detail for the first time. Syngenetic permafrost in the area consists of frozen lagoonal and marine sediments. Massive ice bodies, up to 5.7 m thick, occur in the Holocene deposits of a modern lagoon-sea floodplain and the first terrace and thus obviously have Holocene ages. Patterns of stable isotopes and pollen spectra evidence that the ice is mostly intrasedimental, formed syngenetically in the Late Holocene during freezing of water-saturated ground under intense cryogenic fractionation. Very low δD and $\delta^{18}O$ values in the ice are exceptional for the Holocene ground ice of the Yamal Peninsula.

Massive ice, Holocene, heterogeneity, stable isotopes, heavy oxygen, deuterium, pollen and spores, Yamal Peninsula

INTRODUCTION

This study addresses features of massive ground ice and conditions of its formation in deposits of low lagoon-sea terraces in the northeastern Yamal Peninsula near Sabetta Village (Fig. 1). The territory is remarkable by the presence of widespread massive ground ice within the Holocene first lagoon-marine terrace and the modern layda of the Gulf (Bay) of the Ob River, as well as some such ice in the second terrace.

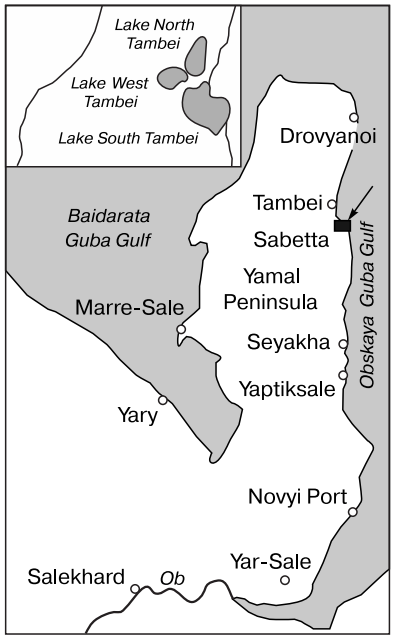

Fig. 1. Location map of Holocene massive ice near Sabetta Village in northeastern Yamal.

Arrow points to study area.

Massive ground ice brings much engineering-geological complexity and poses problems to design, construction, and maintenance of structures. The development of the Sabetta area includes future construction of an international airport, one of world largest in the high latitudes, finishing the construction of a sea port providing year-round navigation along the Northern Sea Route, and setting up industrial and vital infrastructure and facilities. A plant for production, treatment and liquefaction of natural gas will be built on a high layda and on the remnant first lagoon-marine terrace.

Characteristics of Holocene massive ground ice have important implications for its genesis. Pleistocene ice can be of segregated or buried glacier origin [*Solomatin, 2013; Belova, 2014*]. However, no such alternative exists for Holocene ice within subarctic lowlands in northern West Siberia, where no evidence of Holocene ice sheets has been found. Therefore, this massive ice hardly can belong to glaciers but more likely results from segregation or burial of floating or

shore ice. The structures of Holocene massive ice can be a guide in studies of Pleistocene ice of uncertain origin.

Note that Holocene massive ground ice is a very rare phenomenon. In the early 1970s, people from the Tyumen research group of Moscow University stripped a 0.5 m thick layer of ice with a vertical columnar structure in ice-rich floodplain sand in the lower reaches of the Sabettayakha River and interpreted it as ground river ice [*Trofimov et al., 1980, p. 97*].

Elsewhere in Yamal, massive ground ice was encountered among floodplain deposits of the Yuribei River [*Olenchenko and Shein, 2013*], in the first terrace near Kharasavei Village [*Dubikov, 2002*], offshore in the Baidarata Bay and Kara Sea [*Melnikov and Spesivtsev, 1995*], and within the floodplain of the Seyakha (Mutnaya) River and under its bed [*Vasil'chuk, 2012*]. Examples known from other periglacial areas are Holocene massive ground ice in an outcrop near the Slidre River, Eureka Sound area, Fosheim Peninsula (Canada) [*Pollard and Bell, 1998*], and Holocene segregation ice in a sand spit of the Russkiy Zavorot Cape in the Pechora bay shore (northwestern Russia) [*Velikotsky, 2001*]. More widespread are Holocene ice lenses within peatland in different landforms, but their discussion is beyond the present consideration.

LOCATION AND AGE OF STUDIED MASSIVE ICE

The area of the Ob Gulf shore in the Sabettayakha mouth is a terraced swampy tundra with numerous lakes and moss vegetation. There are two terrace levels: the modern lagoon-marine layda (vegetated saline coastal mud flat) and the first lagoon-marine terrace. The layda is composed of Late Holocene alluvial-marine deposits (Fig. 2, *a*), while the first terrace, with a large flat surface of dry thaw lakes (*khasyrei*) at elevations from 4 to 6 m asl, consists of Holocene lagoon-marine sediments (Fig. 2, *b*). The Holocene age of the first terrace in northern Yamal has been confirmed by ^{14}C dates for plant remnants from the base of the first terrace of the Pukhucheyakha River (northwestern Yamal coast, sampling by V.M. Leonov): buried wood samples from depths of 7 m and 4.5 m have ages of 8250 ± 80 yr BP (LU-1139) and 6580 ± 60 yr BP (LU-1138), respectively [*Vasil'chuk et al., 1983*]. The peat base in the first marine terrace in Bely Island from a depth of 2.5 m has an age of 8500 ± 120 yr (LU-1151); and the ages of samples from the first lagoon-marine terrace of the Ob Gulf near Yaptik-Sale Village (collected by A. Vasil'chuk and Yu. Vasil'chuk) from depths 5 m and 4 m are 8960 ± 140 yr BP (MGU-816) and 8700 ± 500 yr BP (MGU-713), respectively. There are young landforms of low-centered polygons, sometimes with swampy lows over wedge ice, on the layda and first terrace surfaces.

LOCAL CLIMATE

The local climate is characterized by a long cold winter with a stable snow cover and a short cold summer. Mean daily air temperatures are positive for up to 109 days and negative for 256 to 265 days. The period of negative daily means lasts eight months, from October to May, and the air temperatures turn to positive values in the first half of June on average. The onset of stable positive mean daily air temperatures in Tambei was the earliest in the middle of May and the latest in the end of June. The mean annual air temperature is –10.2 °C. The territory belongs to the zone of continuous ice-rich permafrost having mean annual temperatures from –1.7 to –6.5 °C.

The area of Sabetta has a complex ice setting with long ice ridges, large hummocks of emerged floating ice (*stamukha*), and shore ice (Fig. 3, *a*). Ice floes are dirty in spring and summer and some show a columnar structure (Fig. 3, *b*).

Fig. 2. First lagoon-marine terrace (*a*) and high layda (*b*). Photograph by A. Amanov.

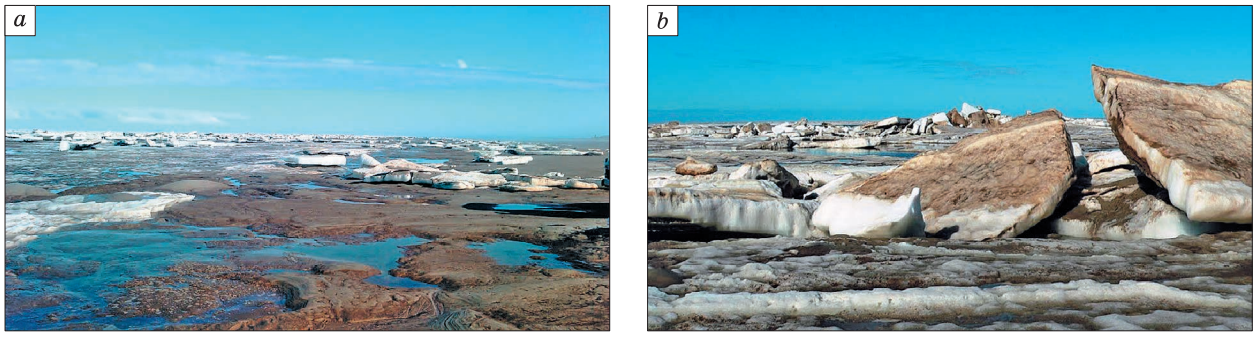

Fig. 3. Remnant shore ice in the summer, emerged during low tide (*a*) and floating ice hummocks (*b*) in the Ob Gulf beach near Sabettayakha mouth. Photograph by A. Amanov.

CRYOSTRATIGRAPHY OF SEDIMENTS AND OCCURRENCE OF MASSIVE GROUND ICE

The layda and first lagoon-marine terrace sections consist mainly of sand in the upper part (more than 50 %) and clay silt in the lower part (about 30 % of the section); silt occupies about 12 % (Fig. 4). The section top is composed of mud: soft deposits of the modern gulf (or lakes in layda), with very high water contents and with plant remnants and humus as an organic component. The lower section contains clay, most often texturally light.

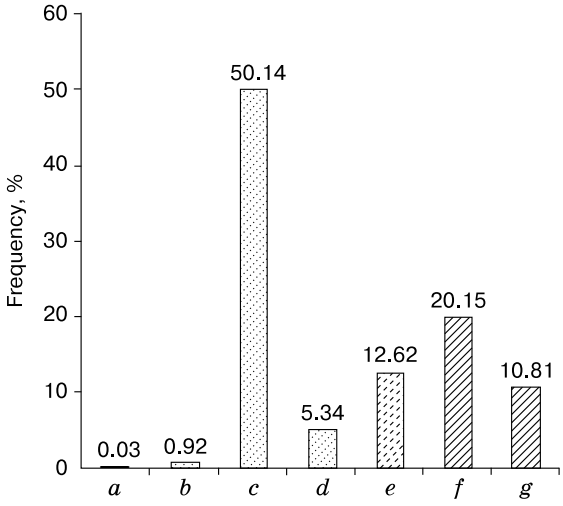

Fig. 4. Main soil types in layda and first lagoon-marine terrace.

a: coarse (gravelly) sand; *b*: medium-grained sand; *c*: fine sand; *d*: silt sand; *e*: silt; *f*: light-textured clay silt; *g*: heavy-textured clay silt.

We investigated the sections of more than 1000 boreholes (BH), from 10 to 100 m deep, in the Ob Gulf coast and encountered massive ground ice in more than 800 holes. Most of ice resides in Holocene lagoonal-marine deposits (Table 1): it is ubiquitous in the upper 10–20 m, which rarely occurs in Holocene sediments. Massive ice lies at different depths, occasionally making a two- to four-stage ice complex (Table 1, Fig. 5).

The ice looks like layers, more or less homogeneous in composition, from a few centimeters to a few meters thick, extending for tens of meters in the lateral dimension. The ice top lies at depths from 0.6 to 21.1 m below the ground surface, and the depth to the base is from 1.6 to 21.4 m. Ice thickness in boreholes varies from 0.2 to 5.7 m, 1.15 m on average. Sometimes there are two, three or even four ice layers in a borehole (Fig. 5, *b*). The ice is commonly non-saline, close to lake or meteoric water.

Massive ground ice occurs in sand-clay, sand, and clay sediments, often at lithological or facies change boundaries (Fig. 5, *a*), but is especially frequent (60 % of cases) in sands. It can lie under sand (59 % of cases), silt (25 %), or silt clay (11 %) and over sand (58 % of cases), silt (26 %), or silt clay (15 %); peat overlies massive ice in 4 % and lies under it only in 0.3 % of cases. Massive ice has been found also in shallow lake bottom sediments.

The ice was documented in greatest detail in three boreholes (BH 12, 17, 42, Table 2; Fig. 6). It was sampled and transported to laboratory in the frozen state, where it was analyzed for stable isotopes, major ions, and spore-pollen contents right after melting.

Table 1. **Average parameters of large Holocene massive ground ice bodies**

Geomorphology	Altitude, m asl	Number of records	Ice thickness, m		
			minimum	average	maximum
First lagoon-marine terrace	5.0–12.0	247	0.1	1.18	5.2
Modern lagoon-marine layda of Ob Gulf	0–5.0	572	0.2	1.08	5.7

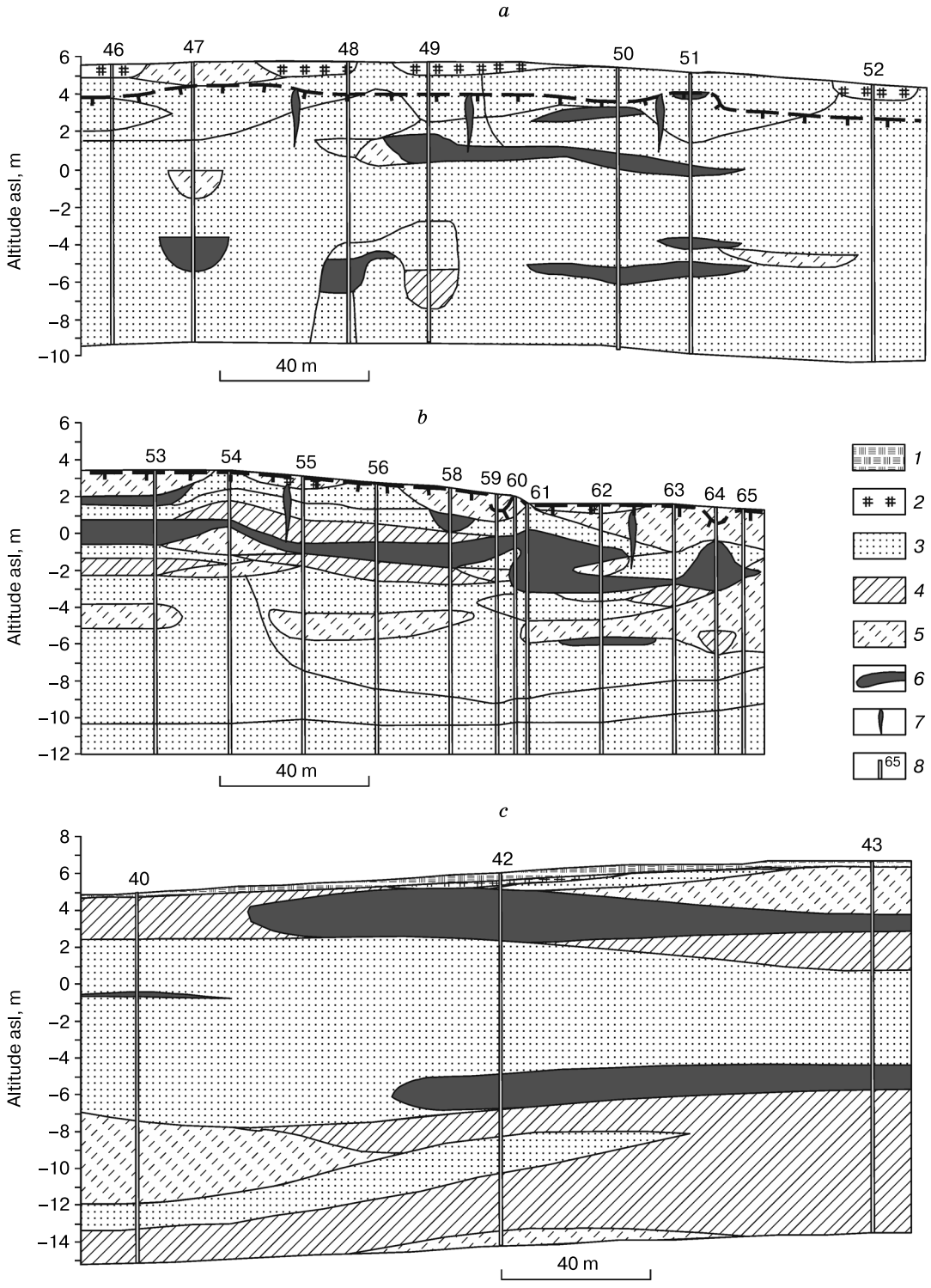

Fig. 5. Boreholes in permafrost with massive ground ice.

1 – moss-vegetation layer; *2* – peat; *3* – sand; *4* – clay silt; *5* – silt; *6* – massive ice; *7* – wedge ice; *8* – borehole and its number.

Table 2. **Cryostratigraphy and cryostructures of Holocene deposits**

Depth, m	Lithology and cryostructures	Ice content
	BH 12, hole top altitude 4.50 m asl	
0–4.0	Fill pad: yellow-gray fine sand; massive cryostructure	Ice-poor
4.0–4.4	Monolith brown ice	98 %
4.4–5.5	Non-saline black silty mud; massive cryostructure	Ice-poor
5.5–7.0	Monolith brown ice, with numerous <1 mm air bubbles, contaminated with fine soil material; prismatic ice crystals	98 %
7.0–20.0	Gray-brown fine sand; low-salinity; organic inclusions; massive cryostructure; light clay silt in intervals 12.0–12.2 and 13.8–14.0 m; silt in intervals 12.8–13.0 and 18.8–19.0 m	Ice-poor
20.0–29.4	Light dark gray clay silt; medium salinity; layered cryostructure, with thin layers of silty sand (to 7 %)	Ice-poor
	BH 17, hole top altitude 1.56 m asl	
0–0.8	Gray clay silt with organic matter (to 10 %)	–
0.8–2.0	Plastic gray silt with organic inclusions	Ice-poor
2.0–5.5	Gray-brown fine sand with thin layers of silty sand; lenticular cryostructure with small lenses	Ice-rich
5.5–6.9	Light brownish gray clay silt; massive cryostructure; poorly degraded peat at depth 6.8–6.9 m	Ice-poor
6.9–9.2	Horizontally layered transparent white ice, with silt (to 1–2 %); large irregularly-shaped ice crystals; enclosed 0.5–1.0 mm air bubbles	100 %
9.2–17.5	Beige-brown fine sand; low salinity; massive cryostructure; ice-rich gray-black clay silt with layered cryostructure at depths 9.2–9.3 m	Ice-poor
17.5–25.0	Dark gray or black heavy clay silt; high salinity; layered cryostructure; enclosed gravel and pebbles (to 5–10 %) and thin layers of light clay in upper section, at 17.5–17.6 m; massive cryostructure with sporadic ice lenses and thin layers of gray silt (to 10–15 %) below 19.5 m	Ice-poor
	BH 42, hole top altitude 5.72 m asl	
0–0.1	Moss-vegetation layer with plant roots	–
0.1–0.3	Strongly degraded brown peat; thinly layered cryostructure, with thin ice lenses	Ice-rich
0.3–0.6	Gray fine sand; organic inclusions; low salinity; massive cryostructure	Ice-poor
0.6–3.4	Brown ice-soil and ice; columnar structure produced by alternated 0.2 to 2 mm thick vertical or oblique ice and soil veins, often slightly curved; mineral soil content 6–8 %	90 %
3.4–10.6	Brown fine sand, with organic matter; low salinity; massive cryostructure; silt at 7.7–8.0 m	Ice-poor
10.6–12.5	White ice with 1–2 % mineral soil	98 %
12.5–13.9	Non-saline heavy clay silt, with organc matter; layered cryostructure, with medium ice lenses	Ice-rich
13.9–16.0	Non-saline brown fine sand; massive cryostructure	Ice-poor
16.0–19.1	Non-saline light dark gay clay silt; layered cryostructure, with thin ice lenses and medium layers; lenses of silty sand (to 10–15 %)	Ice-poor
19.1–20.0	Non-saline brown-gray silt; massive cryostructure	Ice-poor

Ice from BH 42 (Fig. 7, *a*) is brown in the upper part, where it has a columnar structure made by vertical or oblique layers consisting of slightly curved veins intermittent with 0.2 to 2.0 mm soil layers (6–8 % mineral component). Deeper ice (often from the same boreholes) is white and transparent, with horizontal or uncertain layering (Fig. 7, *b*). Massive ice stripped by neighbor boreholes is brown, contaminated with fine-grained sedimentary material (BH 12, Fig. 7, *c*).

We paid special attention to columnar ice in the upper section of some boreholes, as its shallow occurrence might indicate a wedge ice origin. However, this origin is poorly consistent with its structure and texture identified by Professor V.V. Rogov (Fig. 8). The brown columnar ice in the upper section coexists with brown monolith ice, which possibly formed from the same water but in different conditions.

STABLE ISOTOPE RATIOS, MAJOR IONS, AND POLLEN SPECTRA OF ICE

Oxygen and deuterium isotope compositions. The ^{18}O and D ratios were measured in different varieties of massive ground ice: brown monolith, white with horizontal layering, and brown columnar with vertical layers.

The analyses were performed in the Stable isotope laboratory of the Geographical Department of Lomonosov Moscow University on a *Delta-V* mass

spectrometer with the standard gas-bench option. We used the international standards of V-SMOW (Vienna standard mean ocean water, $\delta^{18}O$ = 0 ‰, δD = 0 ‰) and GISP (Greenland Ice Sheet Precipitation, $\delta^{18}O$ = –24.76 ‰, δD = –189.5 ‰), IAEA standards (IAEA-12, $\delta^{18}O$ = –12.10 ‰, δD = = –85.9 ‰; IAEA-13, $\delta^{18}O$ = –33.35 ‰, δD = = –257.2 ‰; and SLAP (Standard Light Antarctic Precipitation), $\delta^{18}O$ = –55.5 ‰, δD = –427.5 ‰), as well as an internal laboratory standard of fresh snow from the Caucasus Garabashi glacier ($\delta^{18}O$ = = –15.60 ‰, δD = –110.0 ‰). The precision was 0.1 ‰ for $\delta^{18}O$ and 0.6 ‰ for δD.

The obtained values are –147.62 to –155.57 ‰ δD and –19.11 to –20.55 ‰ $\delta^{18}O$ in brown ice from borehole 12; –107.1 to –119.8 ‰ δD and –15.73 to –16.06 ‰ $\delta^{18}O$ in horizontally layered white ice from borehole 17; and extremely low δD of –194.5 to –199.7 ‰ at –25.33 to –26.48 ‰ $\delta^{18}O$ in columnar brown ice from borehole 42 (Table 3).

The unusually high differentiation of the oxygen and deuterium isotope ratios is most likely due to cryogenic fractionation in freezing sediments, which is evidence of intrasedimental ice origin, mainly by segregation or by combined processes of ice segregation and water intrusion. It is also possible that ice involves waters of different types, such as extremely cold winter precipitation in columnar ice and lake water for white and brown ice.

Major ions. The concentrations of major ions were analyzed by ion chromatography in ice samples right after their melting (Table 4) and compared with those in newly collected samples of snow, ice and sea water determined in the same runs.

Type 1: ultra-fresh (<200 mg/l) columnar brown ice, with 40.64 mg/l mineral content, Cl^-, SO_4^{2-}, Mg^{2+} ion composition, and pH = 7.9.

Type 2: ultra-fresh white ice with horizontal layering, with the least mineralization of all samples (10.92–13.52 mg/l), Cl^-, Mg^{2+} and Cl^-, Ca^{2+} ion composition, and pH = 8.00–8.01.

Type 3: ultra-fresh and fresh monolith brown ice, with 81.9–229.28 mg/l mineralization, Cl^-, Na^+ ion composition, and pH = 6.7–7.5. Another sample of this ice showed high mineral contents of 229 mg/l, apparently because it was contaminated with soil.

Electrical conductivity used to estimate concentrations of dissolved salts (TDS) was the highest in monolith brown ice (233.0–661.01 μS/cm), like mineralization, but it was 102.5 μS/cm in columnar brown ice and 13.5–18.98 μS/cm in white ice. TDS in all samples are relatively low and approach the values of meteoric and fresh surface (lake and river) waters, e.g., Moscow snow and Baikal ice, with 15.45 to 203 and 25.6 μS/cm, respectively. The analyzed ice varieties are much less saline than marine ice of the White Sea or even than snow on its surface (992.4–2750.6 mg/l; 1944–5420 μS/cm).

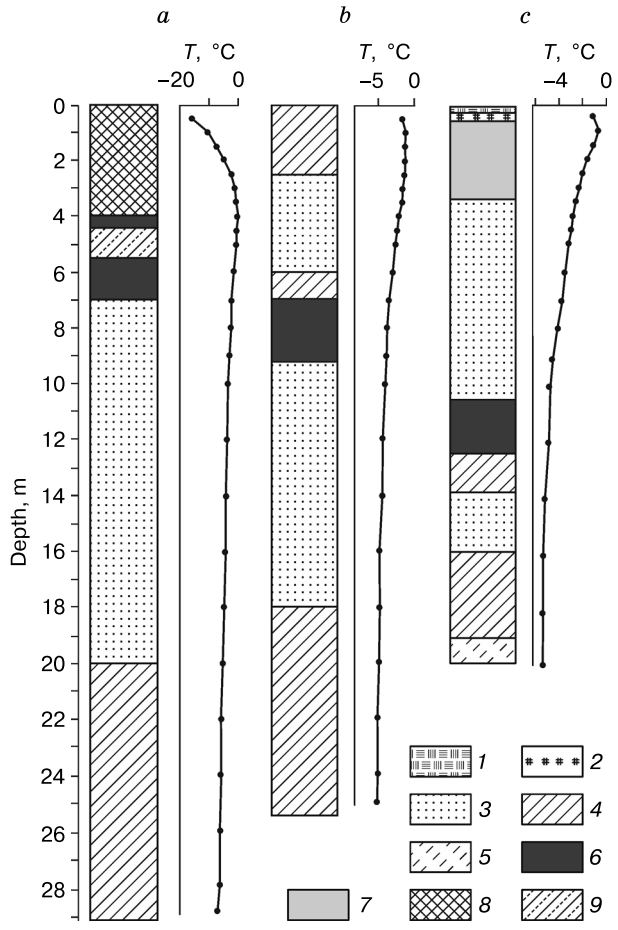

Fig. 6. Stratigraphy of first lagoon-marine terrace and layda with massive ice.

a: BH 12, *b*: BH 17, *c*: BH 42; *1* – moss-vegetation layer; *2* – peat; *3* – sand; *4* – clay silt; *5* – silt; *6* – horizontally layered white ice; *7* – columnar brown ice; *8* – soil pad; *9* – black mud.

The most strongly mineralized Cl^-, Na^+ composition of type 3 brown ice indicates influence of the Baidarata and Ob gulf waters.

The ***pollen spectra*** of soil-contaminated brown columnar ice contain abundant alder pollen, some amounts of dwarf birch, sedge, and heath pollen, as well as spores of green and sphagnum mosses and equisetum. Most of pollen grains are poorly preserved, and are often coated with clay particles, which most likely belong to the host sediments (Table 4). These pollen spectra are similar to those of Holocene sediments, floodplain and layda deposits from the Tambei-Sabettayakha coast of Yamal [*Vasil'chuk A.K., 2005, 2007*]. Therefore, ice obviously formed in the Holocene.

The pollen spectra in columnar brown ice and horizontally layered white ice are similar, with predominant shrub pollen of dwarf birch and alder (37–52 %). Pollen and spores in both ice varieties are un-

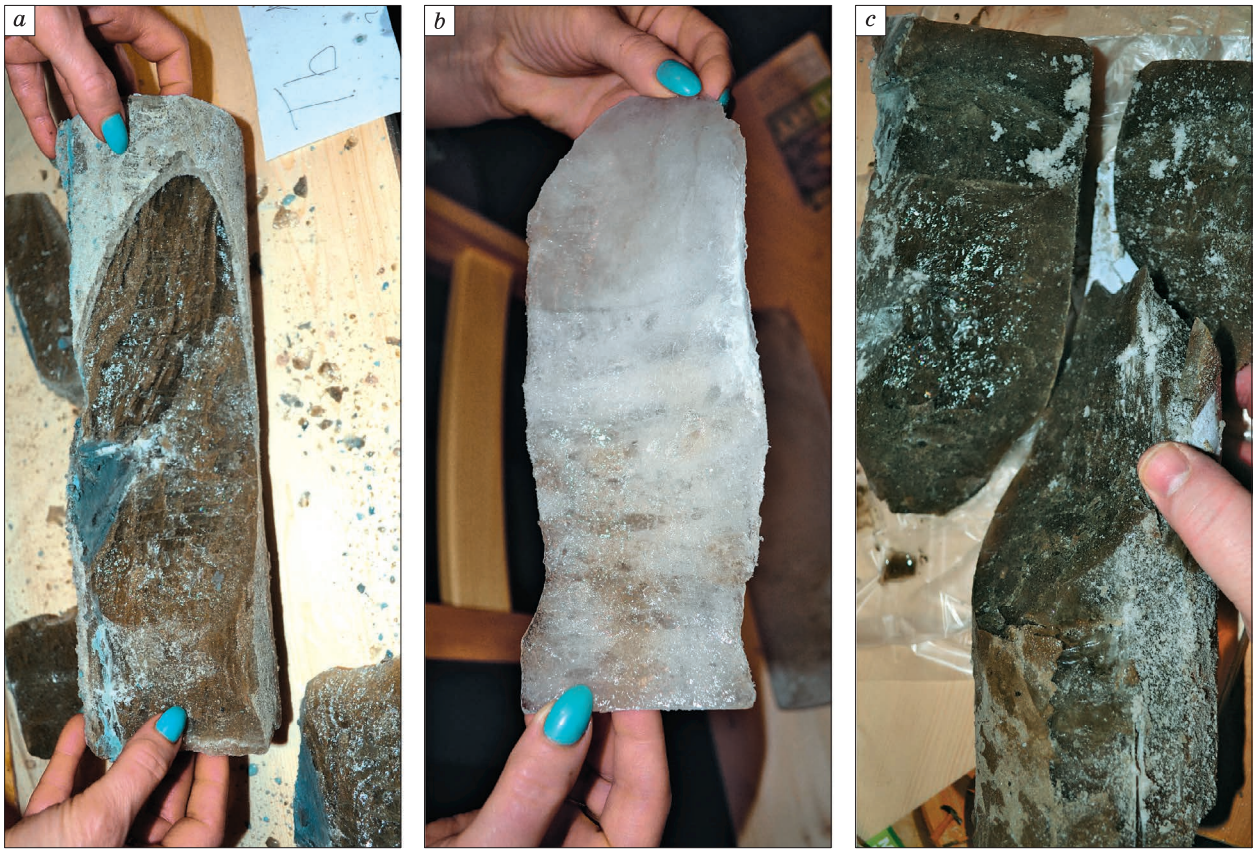

Fig. 7. Types of Holocene massive ice near Sabettayakha mouth. Photograph by Yu.K. Vasil'chuk.
a: columnar brown ice, BH 42; *b*: horizontally layered white ice, BH 17; *c*: monolith brown ice, BH 12.

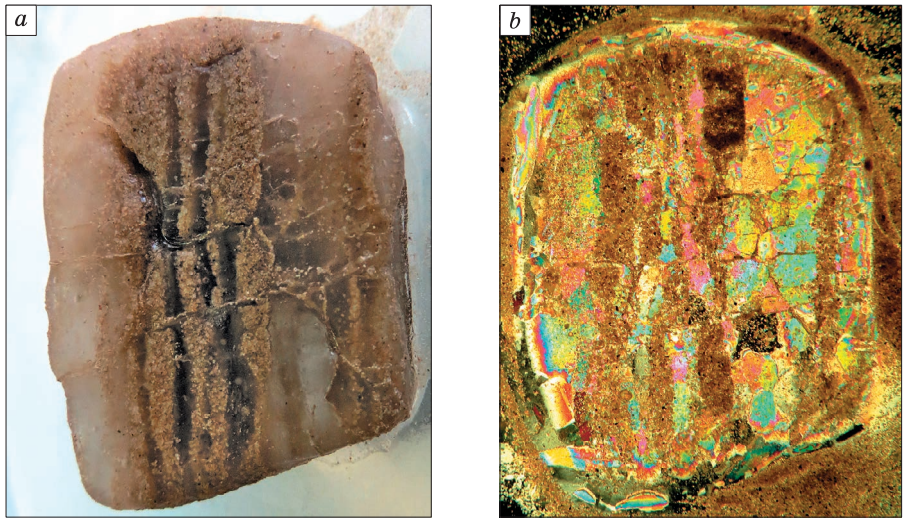

Fig. 8. Texture (*a*) and structure (*b*) of Holocene columnar brown ice from BH 42.
Polarized light. Photograph by V.V. Rogov.

Table 3. **δD, $\delta^{18}O$ and d_{exc} values in different ice types**

Number	δD	$\delta^{18}O$	d_{exc}	Number	δD	$\delta^{18}O$	d_{exc}
	‰				‰		
BH 12, depth 6.5–6.8 m, monolith brown ice				*BH 42, depth 1.3–1.6 m, columnar brown ice*			
12/1	–150.4	–19.98	9.44	42/8	–197.6	–26.07	10.96
12/2	–147.6	–19.11	5.28	42/9	–194.8	–25.92	12.56
12/3	–152.8	–20.21	8.88	42/10	–194.7	–25.76	11.38
12/4	–155.6	–20.19	5.92	42/11	–193.4	–26.04	14.92
12/5	–151.8	–20.55	12.60	42/12	–192.7	–25.33	9.94
12/6	–149.7	–20.22	12.06	42/18	–193.8	–26.24	16.12
12/7	–154.5	–20.18	6.94	42/19	–196.5	–26.12	12.46
BH 17, depth 8.3–8.5 m, transparent white ice				42/20	–198.5	–26.46	13.18
17/13	–107.1	–15.77	19.09	42/21	–197.2	–26.25	12.80
17/14	–110.5	–15.79	15.82	42/22	–198.3	–26.12	10.66
17/15	–114.2	–16.02	13.96	42/23	–197.2	–26.01	10.88
17/16	–113.5	–16.06	14.98	42/24	–194.5	–25.65	10.70
17/17	–114.9	–15.74	11.02	42/25	–194.5	–26.07	14.06
17/32	–115.3	–15.89	11.82	42/26	–196.2	–26.24	13.72
17/33	–112.5	–15.87	14.46	42/27	–199.3	–26.23	10.54
17/34	–119.8	–15.73	6.04	42/28	–198.6	–26.36	12.28
17/35	–118.8	–15.80	7.60	42/29	–199.7	–26.28	10.54
17/36	–113.2	–15.57	11.36	42/30	–197.2	–26.48	14.64
17/37	–112.9	–15.62	12.06	42/31	–199.7	–25.98	8.14

Table 4. **Major ions (equivalent %), mineralization (M, mg/l) and contents of total dissolved solids derived from conductivity (TDS, μS) in the Sabettayakha Holocene ice, compared to those in newly molten snow, ice and sea water samples**

Sampling site	pH	M	TDS	HCO_3^-	Cl^-	SO_4^{2-}	NO_3^-	Ca^{2+}	Mg^{2+}	Na^+	K^+
Sabettayakha R., BH 42, depth 0.6–3.4 m, columnar brown ice	7.9	40.64	102.5	29.14	34.53	35.92	0.41	10.96	51.37	29.93	7.74
Sabettayakha R., BH 17, depth 6.9–9.2 m, white ice, sample 38	8.01	10.92	18.98	33.08	55.67	11.25	0.00	42.95	9.34	35.37	12.34
Same site, BH 17(60), sample 39	8.0	13.52	13.5	25.87	55.61	16.92	1.60	7.54	66.05	20.61	5.80
Sabettayakha R., BH 12, depth 5.5–7.0 m, monolith brown ice, sample 8	7.5	81.9	233	21.85	70.62	7.25	0.28	10.16	38.14	47.80	3.90
Same site, sample 9 (soil contaminated)	6.7	229.28	661.01	23.09	75.80	1.11	0.00	21.24	20.64	55.96	2.16
Moscow snow (sample 5/1)	6.7	12.2	15.45	55.40	33.64	6.18	4.78	56.19	6.16	32.32	5.33
New snow (Moscow, 03.02.2015)	7.11	55.08	203	25.55	65.43	6.22	2.80	24.14	6.95	53.90	15.01
Baikal ice	6.81	11.68	25.6	86.30	11.43	2.27	0.00	90.23	0.89	5.70	3.18
White Sea, new snow (sample 010)	6.56	992.4	1944	0.00	88.08	11.92	0.00	7.26	17.98	70.22	4.54
Same site, ice, depth 0–5 cm (sample 016)	6.69	2750.6	5420	0.00	87.22	12.78	0.00	7.92	16.53	73.81	1.74
Same site, ice, depth 15–20 cm (sample 011)	6.79	2647.75	5410	0.00	88.24	11.76	0.00	8.13	17.11	72.81	1.95
Same site, ice, depth 20–27 cm (sample 012)	6.58	2388.7	4200	0.00	87.89	12.11	0.00	7.25	17.44	72.85	2.46
White Sea, sub-ice water (sample 001)	7.31	26 599.3	40 000	0.00	86.62	13.38	0.00	3.88	16.39	78.00	1.73

Table 5. **Spore and pollen spectra (%) in the Sabettayakha ice, compared with those from modern and Holocene cryogenic objects and Pleistocene wedge ice**

Spores and pollen	Massive ice								Snow fields and wedge ice				
	Tambei gas-condensate field					Yamal and Gydan Peninsulas							
	1	*2*	*3*	*4*	*5*	*6*	*7*	*8*	*9*	*10*	*11*	*12*	*13*
Tree pollen	8.8	–	–	1*	7.1	–	–	7	12.3	12.4	14.3	52	5
Shrub pollen	52.6	–	19*	–	37.5	43	36.4	39	1.5	15.1	26.7	4	35
Grass and low shrub pollen	11.4	–	–	–	33.9	16	29.9	32	46.0	32.3	53.7	28	37
Spores	27.2	2*	10*	1*	21.4	41	33.7	22	40.2	40.3	5.3	16	23
Picea	–	–	–	–	–	–	–	–	–	–	–	20	–
Pinus sibirica	–	–	–	–	–	–	–	–	1	5.9	6	20	1
Pinus sylvestris	1.8	–	–	–	–	–	–	–	–	–	–	–	–
Alnus	1.8	–	–	–	–	–	–	–	1	–	0.6	–	–
Betula	5.3	–	–	1*	7.1	–	–	7	8.8	6.5	7.7	12	4
Betula sect. *Nanae*	22.8	–	19*	–	21.4	28	27. 3	22	1.5	11.2	12.4	4	27
Alnaster	29.8	–	–	–	16.1	15	6.5	3	–	3.8	3.0	–	3
Salix	–	–	–	–	–	–	2.6	14	–	–	11.3	–	5
Poaceae	–	–	–	–	–	9	–	11	23.7	13.5	19.6	4	26
Cyperaceae	7.0	–	–	–	25.0	3	–	20	13.3	13.0	24.0	–	6
Ericaceae	4.4	–	–	–	5.4	–	28.6	–	4.5	2.1	6.5	4	3
Varia	–	–	–	–	–	2	–	–	–	3.0	1.8	20	1
Chenopodiaceae	–	–	–	–	3.6	–	1.3	–	1	–	–	–	–
Artemisia	–	–	–	–	–	2	–	1	1	0.5	1.8	–	1
Bryales	8.8	1*	10*	1*	14.3	31	1.3	22	32.7	16.6	1.8	8	10
Sphagnum sp.	12.3	1*	–	–	7.1	8	31.1	–	3.2	–	2.9	8	3
Polypodiaceae	3.5	–	–	–	–	2	1.3	–	1.3	–	–	–	–
Equisetum sp.	2.6	–	–	–	–	–	–	–	–	23.7	–	–	10
Huperzia selago	–	–	–	–	–	–	–	–	0.5	–	0.6	–	–
Reworked, %	3	–	–	–	–	24.5	–	–	4.8	–	2.0	–	–
Concentration, grains/l	361	6	87	6	168	125	177	306	270	389	364	100	457

Note. Numbers on top: *1* – columnar brown ice, Sabettayakha, sample 42/11; *2* – columnar brown ice, Sabettayakha, sample 42/12; *3* – white transparent ice, Sabettayakha, sample 17/14; *4* – white transparent ice, Sabettayakha, sample 17/16; *5* – white transparent ice, Sabettayakha, sample 17/17; *6* – massive ice, Kharasavei Cape; *7* – massive ice, upper reaches of Mordyyakha River; *8* – massive ice, mouth of Gyda River; *9* – snow field, Matyui-Sale Village; *10* – snow field, Gyda River; *11* – ice, Ob gulf coast near Gyda Village; *12* – Late Holocene wedge ice, mouth of Tambei River; *13* – Holocene wedge ice, Matyui-Sale Village.

* Denotes number (not percentage) of pollen grains and spores.

evenly distributed: 300 grains/l in some samples (Nos. 1, 5, Table 5) and almost zero in others (samples 2, 4, Table 5), the contents in white transparent ice being slightly lower than in brown ice. Columnar brown ice contains more pollen grains of *Betula*, *Alnaster*, and Poaceae with clay coating that come from the sedimentary host. However, some layers in white transparent ice contain only coated pollen grains, e.g., a single clay-coated grain of *Betula* in sample 4 (Table 5).

Sample 42/11 shows strongly damaged spectra of reworked pollen and contains round 10 μm grains of soil. Note fragments of organic components in sample 42/12; absence of organic matter in 17/14; a clay-coated *Betula* grain in 17/16; and small rounded quartz grains in 17/17 (Table 5).

HETEROGENEITY OF MASSIVE GROUND ICE

Two features of the structure and composition of the Sabettayakha Holocene massive ground ice are worth special attention. First, it is the presence of brown ice with a distinct columnar structure produced by alternation of thin (less than 1 cm) vertical layers of brown ice and sand, in addition to horizontally layered white and monolith brown ice. Second, high contrasts in stable isotope ratios in different ice types: more than 10 ‰ in $\delta^{18}O$ and 90 ‰ in δD. The δD range is from –107.1 ‰ in white ice to –199.7 ‰ in brown columnar ice, and that of $\delta^{18}O$ is from –15.73 to –26.48 ‰, respectively.

If the low isotope ratios in columnar brown ice from the upper section had referred to Pleistocene

ice, burial of strongly deformed glacier ice would have been a passable hypothesis. However, Late Pleistocene ice of this kind is known [*Vasil'chuk et al., 2009, 2011*] to contain remnants of lake algae and tundra pollen spectra, which actually rules out the glacier origin. The columnar massive ice found in the Holocene lagoon-marine layda at the Sabettayakha mouth cannot be derived from a glacier, and its structure must have some other cause. Note that columnar structure was often reported [*Vasil'chuk et al., 2009, 2011, 2012*] for Late Pleistocene ice bodies from the Bovanenkovo, Erkutayakha and Mordyyakha valleys. There is a morphological analogy with columnar ice from the upper part of the Marre-Sale section described by *Slagoda et al.* [*2012, Fig. 5, B*].

The difference in the $\delta^{18}O$ and δD values of ice bodies from the same sections, especially that exceeding 4–5 ‰ in $\delta^{18}O$ and 30–40 ‰ in δD, can provide additional constraints on ice genesis. To be fair, such cases are very rare, but the case of the Sabettayakha Holocene sediments is just one of these. The strongly depleted $\delta^{18}O$ and δD ratios in the columnar brown ice we analyzed are 10 ‰ lower in $\delta^{18}O$ and almost 90 ‰ lower in δD than the respective values in white ice (Fig. 9, *A*). This difference would prompt different mechanisms of ice formation, but we observed a still greater contrast in homogeneous lenses of ground ice in the Gyda River valley (Fig. 9, *B*) [*Vasil'chuk et al., 2001*]. It was, namely, 18 ‰ in $\delta^{18}O$ produced by very strong cryogenic isotope fractionation upon segregation during freezing of alluvium with high moisture contents in a closed system without water recharge. The same fractionation during the segregation process may be responsible for the isotopic contrasts in the Sabettayakha massive ground ice from Holocene lagoonal-marine deposits.

Strongly depleted isotope ratios reaching –199.7 ‰ δD and –26.48 ‰ $\delta^{18}O$ in columnar brown ice are exceptional for the Holocene ground ice in Yamal, as well as for more depleted Late Pleistocene ice in West Siberia [*Vasil'chuk, 2013; Vasil'chuk and Vasil'chuk, 2014*]. Note that values of no lower than –25 ‰ $\delta^{18}O$ and –189 ‰ δD were obtained in the Seyakha wedge ice formed from winter snow during the Late Pleistocene cryochron [*Vasil'chuk, 1992, 2006*]. Other examples are: Late Pleistocene massive ice in Yamal in the Erkutayakha valley, with –149.6 to –172.7 ‰ δD and –19.24 to –23.42 ‰ $\delta^{18}O$ [*Vasil'chuk et al., 2011*]; ice bodies in the upper reaches of the Mordyyakha River, with the ranges –164.8 to –172.9 ‰ δD and –21.0 to –23.3 ‰ $\delta^{18}O$ [*Vasil'chuk et al., 2012*]; ice bodies within the Bovanenkovo gas-condensate field with –91.7 to –177.1 ‰ δD and –12.49 to –23.13 ‰ $\delta^{18}O$ [*Vasil'chuk et al., 2009, 2014*]. Other Yamal and Gydan Late Pleistocene bodies of massive ice studied recently neither reach the oxygen and heavy hydrogen isotope depletion of the Sabettayakha ice [*Vasil'chuk, 2012, 2014; Belova, 2014*]. Namely, they are no lower than –197.5 ‰ δD and –26.26 ‰ $\delta^{18}O$ near Kharasavei Village; –163.6 ‰ δD and –25.5 ‰ $\delta^{18}O$ in the Oyuyakha valley; –190.6 ‰ δD and –24.8 ‰ $\delta^{18}O$ in the Marre-Sale section, both in massive ice and in Late Pleistocene wedge ice [*Romanenko, 2001; Slagoda et al., 2012; Streletskaya et al., 2013*]. The $\delta^{18}O$ values remain no lower than –23.5 ‰ even in Ledyanaya Gora thick massive ice in the Yenisei valley [*Vaikmae et al., 1993*].

A more depleted $\delta^{18}O$ composition of ice in northern West Siberia, with the range from –16.2 to –34.3 ‰, is known only for ice lenses in the Gyda mouth which result from cryogenic fractionation during formation of intrasedimental ice, by infiltration and segregation [*Vasil'chuk, 1992; Vasil'chuk et al., 2001*]. This fractionation may be responsible for depleted isotope ratios in the columnar brown ice from BH 42. Note that the host sand is highly saline, while the ice is non-saline and isotopically depleted. Another hypothesis, of a small but not zero probability, is burial of shore ice floes consisting of ultra-depleted winter snow, like the case of Fig. 3, *b*. Such burial may be due to a catastrophic spring surge and ice jam in the Ob Gulf that brought a large amount of sand.

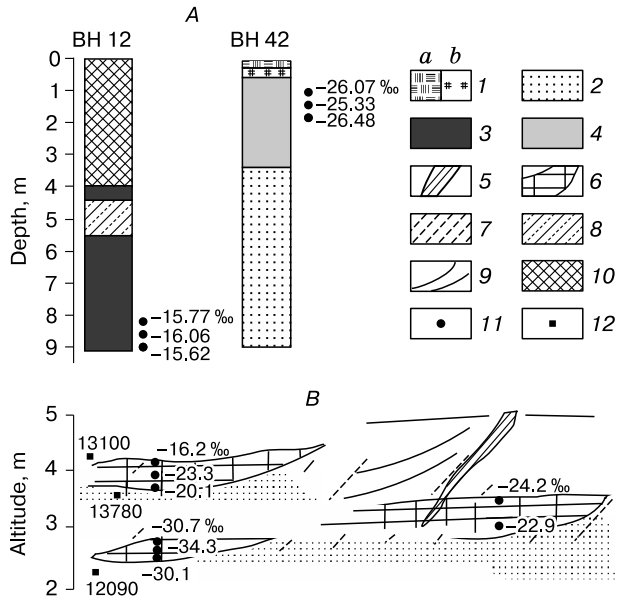

Fig. 9. Variations of $\delta^{18}O$ (‰) in massive ground ice in first lagoon-marine terrace (*A*) near Sabettayakha mouth and first alluvial terrace (*B*) in Gydan.

1 – peat (*a*), plant roots and scattered litter (*b*); *2* – sand; *3* – horizontally layered white ice; *4* – columnar brown ice; *5* – syngenetic Late Pleistocene wedge ice; *6* – lens-like massive ice; *7* – silt; *8* – black silt; *9* – sedimentary bedding; *10* – sand fill pad; *11, 12* – sampling points for $\delta^{18}O$ (*11*) and ^{14}C (*12*) analyses.

Oxygen isotope composition of sea ice in different areas of the Russian Arctic can differ from that of sea water, namely measured as (i) −0.6 ‰ $\delta^{18}O$ in ridges of sea ice near Kharasavei Village (71°06′ N, 66°45′ E) in western Yamal in January 1984; (ii) −1 ‰ $\delta^{18}O$ in floating sea ice near Matyui-Sale Village (71°47′ N, 76°49′ E) in the northern Gydan Peninsula in August 1983; (iii) −1.9 ‰ $\delta^{18}O$ in sea ice near Ayon Island (69°47′ N, 168°39′ E) in July 1986, the sea water value at the same site being −8.9 ‰ [*Vasil'chuk and Vasil'chuk, 2011*].

The coexistence of *Equisetum* spores with notable amounts of Cyperaceae pollen in columnar ice may indicate a lake-bog origin of the source water coming from a sub-lake talik. Generally, the pollen spectra correspond to those of Arctic tundra, i.e., to modern landscapes. Rounded spherical 10–60 μm quartz grains present in the ice were likely transported by water. White horizontally layered ice from BH 17, with very low spore and pollen contents, stores perfectly preserved dwarf birch pollen grains.

Importantly, pollen grains in brown columnar ice are poorly preserved and are often coated with clay, i.e., spores and pollen come from the host sediments. The presence of *Equisetum* spores in massive ice is evidence of water recharge from thaw lakes and bogs. On the other hand, the dwarf birch pollen with vacuoles that survived in white layered ice have not been reworked but fell either into water (e.g., the birch grew near a shallow lake or a river) which froze soon after that, or into early snow which prevented the fluid-filled vacuoles from transformation.

The pollen spectra from horizontally layered transparent ice are the most similar in the structure and percentages of components to those from wedge ice in the Mammoth Peninsula lying about 170 km northeast of the Sabettayakha mouth (Table 5, sample 13). However, there is no similarity with the pollen spectra of wedge ice located much nearer, only 30 km away, in the Tambei mouth (Table 5, sample 12). The wedge ice contains high percentages of cedar pine, spruce, birch, and grasses [*Vasil'chuk, 2005*], the species almost absent from the Sabettayakha massive ice.

Comparison of the Sabettayakha ice pollen spectra with those from other massive ice bodies we studied in the Kharasavei Cape, in the upper reaches of the Mordyyakha, and in the Gyda mouth shows high percentages of shrub pollen in all cases: 32–53 % in the Sabettayakha ice and 36–43 % in ice from elsewhere. *Alnaster* pollen is more frequent in Sabettayakha than elsewhere (16–29 %) while *Betula* sect. *Nanae* pollen is 19.0–22.8 %. There are few grains of *Pinus sylvestris* pollen, which was transported from distant places but likely became soon conserved in the ice judging by its very good preservation. Note that the Sabettayakha ice almost lacks grass pollen which is frequent on the surface of snow fields and in Holocene wedge ice (Table 5, samples 9–13), but it likely contains pollen brought by late autumn-winter pollen rains.

Holocene massive ground ice is important for geocryology as its structures and textures can be used as a guide in studies of older ice bodies of uncertain origin. The Sabettayakha Holocene ice is undoubtedly heterogeneous. It may be a combination of segregation and intrusive-segregation ice, or some layers may be produced by catastrophic burial of shore ice, floating ice hummocks, or lake ice. The probability of floating ice burial in lake basins follows from the upside down position of ice bodies reaching 10 m high and 100–200 m long in this part of the Ob Gulf [*Kubyshkin et al., 2014*].

CONCLUSIONS

The key results of the reported studies can be summarized as follows.

1. Drilling in the Ob Gulf coast near the Sabettayakha mouth stripped unique Holocene massive ground ice in syngenetically frozen lagoonal-marine deposits of a modern high layda and the first sea terrace. Massive ice is common to Holocene sediments elsewhere but is an unusual and exceptionally rare phenomenon in the area. The Holocene age of the ice, reaching a thickness of 5.7 m, is inferred from its occurrence in Holocene deposits.

2. The oxygen and heavy hydrogen isotope compositions and spore-pollen spectra of the Holocene massive ground ice have implications for its genesis. The Sabettayakha ice obviously cannot have a glacier origin.

3. Stable isotope ratios in the analyzed ice samples show large ranges of −107.0 to −199.7 ‰ δD and −15.7 to −26.48 ‰ $\delta^{18}O$. The patterns are different in three types of ice: (a) −147.62 to −155.57 ‰ δD and −19.11 to −20.55 ‰ $\delta^{18}O$ in monolith brown ice; (b) −107.1 to −119.8 ‰ δD and −15.73 to −16.06 ‰ $\delta^{18}O$ in horizontally layered white ice; and (c) extremely depleted values of −194.5 to − 199.7 ‰ δD and −25.33 to −26.48 ‰ $\delta^{18}O$ in columnar brown ice contaminated with soil. Such isotope differentiation must result from cryogenic fractionation in freezing sediments. The most depleted isotope values in the Holocene ice are lower than in Late Pleistocene wedge ice of Yamal.

4. Pollen grains in columnar brown ice most likely came from the host sediments, judging by their poor preservation and clay coating. The presence of Equisetum pollen in massive ice is evidence of its possible thaw lake or bog water source.

5. Pollen grains in horizontally layered white ice experienced neither reworking nor distant transport: their perfect preservation (dwarf birch pollen with survived vacuoles) indicates that they fell into snow or into ice which froze up immediately after that.

6. The structures and textures of Holocene massive ground ice can be used as a guide in studies of older ice bodies of uncertain origin. The Sabettayakha massive ice is obviously heterogeneous and appears to be an intrasedimental segregation ice combined with intrusive-segregation ice. Some layers may result from catastrophic burial of shore ice, floating ice hummocks, or lake ice. The probability of floating ice burial in lake basins follows from the upside down position of ice bodies.

We wish to thank Professor V.V. Rogov for analysis of ice structures and textures and J. Vasil'chuk, E.V. Terskaya, and L.V. Dobrydneva for analytical work. We greatly appreciate constructive criticism by Professor V.T. Trofimov and discussions with Professor S.M. Fotiev and Doctor E.A. Slagoda.

The study was supported by grant 14-27-00083 from the Russian Science Foundation.

References

Belova, N.G., 2014. Massive Ice in the Southwestern Kara Sea Coast. MAKS Press, Moscow, 180 pp. (in Russian)

Dubikov, G.I., 2002. Lithology and Cryostratigraphy of Sediments in West Siberia. GEOS, Moscow, 246 pp. (in Russian)

Kubyshkin, N.V., Vinogradov, R.A., Gudoshnikov, Yu.P., Nesterov, A.V., Andreev, O.M., 2014. Comprehensive meteorological studies in the northern Ob Gulf for development of the South Tambei gas-condensate field, in: Proc. Tenth Russian Conf. of Prospecting Groups, Akadem. Nauka, Moscow, pp. 133–134. (in Russian)

Melnikov, V.P., Spesivtsev, V.I., 1995. Engineering-geological and permafrost conditions of the Barents and Kara Shelves. Nauka, Novosibirsk, 198 pp. (in Russian)

Olenchenko, V.V., Shein, A.N., 2013. Possibilities of geophysical methods in the search for Pleistocene megafauna in floodplain and above floodplain deposits of the Yuribey river (Yamal). Kriosfera Zemli XVII (2), 83–92.

Pollard, W., Bell, T., 1998. Massive ice formation in the Eureka Sound Lowlands: A landscape model. Permafrost: Proc. of the Seventh Intern. Conf. Yellowknife, Canada, Univ. Laval, pp. 903–908.

Romanenko, F.A., 2001. Formation of Massive Ice in Western Yamal, in: Proc. Second Conf. of Russian Permafrost Scientists (Moscow, 6–8 June 2001), Moscow University Press, Moscow, Book 1, Part 2, pp. 247–253. (in Russian)

Slagoda, E.A., Opokina, O.L., Rogov, V.V., Kurchatova, A.N., 2012. Structure and genesis of the underground ice in the Neopleistocene-Holocene sediments of Marre-Sale cape, Western Yamal. Kriosfera Zemli XVI (2), 9–22.

Solomatin, V.I., 2013. Physics and Geography of Ground Ice. Geo Publishers, Novosibirsk, 346 pp. (in Russian)

Streletskaya, I.D., Vasiliev, A.A., Oblogov, G.E., Matyukhin, A.G., 2013. Isotope geochemistry of ground ice in Western Yamal (Marre-Sale). Led i Sneg, No. 2 (122), 83–92.

Trofimov, V.T., Badu, Yu.B., Dubikov, G.I., 1980. Cryostratigraphy and ice contents of permafrost in the West Siberian Plate. Moscow University Press, Moscow, 245 pp. (in Russian)

Vaikmae, R.A., Michel, F.A., Solomatin, V.I., 1993. Morphology, stratigraphy and oxygen isotope composition of fossil glacier ice at Ledyanaya Gora, Northwest Siberia, U.S.S.R. Boreas 22, 205–213.

Vasil'chuk, A.C., 2005. Formation of Pollen Spectra in the Russian Permafrost Zone. Moscow University Press, Moscow, 245 pp. (in Russian)

Vasil'chuk, A.C., 2007. Palynology and chronology of wedge ice complexes in the Russian Permafrost Zone. Moscow University Press, Moscow, 488 pp. (in Russian)

Vasil'chuk, Yu.K., 1992. Oxygen isotope composition of ground ice (application to paleogeocryological reconstructions). Theoretical Problems Department. The Russian Academy of Sciences, Geological Faculty of Moscow University, Research Institute of Engineering Site Investigations. Moscow; Vol. 1 – 420 pp. Vol. 2 – 264 pp. (in Russian).

Vasil'chuk, Yu.K., 2006. Ice Wedge: Heterocyclity, Heterogeneity, Heterochroneity. Moscow University Press, Moscow, 404 pp. (in Russian).

Vasil'chuk, Yu.K., 2012. Isotope Methods in the Environment. Part 2: Stable Isotope Geochemistry of Massive Ice. Moscow University Press, Moscow, Vol. I, 472 pp. (in Russian)

Vasil'chuk, Yu.K., 2013. Syngenetic ice wedges: cyclical formation, radiocarbon age and stable-isotope records. Permafrost and Periglacial Processes 24 (1), 82–93.

Vasil'chuk, Yu.K., 2014. Isotope Methods in the Environment. Part 2: Stable Isotope Geochemistry of Massive Ice. Moscow University Press, Moscow, Vol. II, 244 pp. (in Russian)

Vasil'chuk, Yu.K., Budantseva, N.A., Vasil'chuk, A.C., 2011. Variations in $\delta^{18}O$, δD, and the concentration of pollen and spores in an autochthonic heterogeneous massive ice on the Erkutayaha River in the southern part of the Yamal Peninsula. Doklady Earth Sciences 438(1), 721–726.

Vasil'chuk, Yu.K., Petrova, E.A., Vasil'chuk, A.C., 1983. Some features of Holocene paleogeography of Yamal Peninsula. Bull. Comission on Quaternary 52, 73–89.

Vasil'chuk, Yu.K., Vasil'chuk, A.C., 2011. Isotope Methods in the Environment. Part 1: Stable Isotope Geochemistry of Natural Ice. Moscow University Press, Moscow, 228 pp. (in Russian)

Vasil'chuk, Yu., Vasil'chuk, A., 2014. Spatial distribution of mean winter air temperatures in Siberian permafrost at 20–18 ka BP using oxygen isotope data. Boreas 43 (3), 678–687.

Vasil'chuk, Yu.K., Vasil'chuk, A.C., Budantseva, N.A., 2012. Isotopic and palynological compositions of a massive ice in the Mordyyakha River, Central Yamal Peninsula. Doklady Earth Sciences. 446(1), 1105–1109.

Vasil'chuk, Yu.K., Vasil'chuk, A.C., Budantseva, N.A., Chizhova, Ju.N., Papesch, W., Podborny, Ye.Ye., Sulerzhitsky, L.D., 2009. Oxygen Isotope and Deuterium Indication of the Origin and ^{14}C Age of the Massive Ice, Bovanenkovo, Central Yamal Peninsula. Doklady Earth Sciences 429(8), 1326–1332.

Vasil'chuk, Yu.K., Vasil'chuk, A.C., Budantseva, N.A., Chizhova, Ju.N., Papesch, W., Podborny, Ye.Ye., 2014. ^{14}C age, stable isotope composition and pollen analysis of massive ice, Bovanenkovo gas field, Central Yamal Peninsula. Geography, Environment, Sustainability 7 (2), 49–70.

Vasil'chuk, Yu.K., Vasil'chuk, A.C., Chizhova, Yu.N., Budantseva, N.A., 2001. Anomalies in $\delta^{18}O$ and δD patterns in the highland and permafrost snow cover. Materialy Glaciol. Issled. 91, 34–42.

Velikotsky, M.A., 2001. Massive ice in sand spits of the Pechora sand bar, in: Solomatin, V.I. (Ed.), Problems of General and Applied Geo-environment of the North, Moscow University Press, Moscow, pp. 148–154. (in Russian)

Received January 12, 2015